

## BEAM INSTRUMENTATION FOR THE SUPERKEKB RINGS

M. Arinaga, J. W. Flanagan, H. Fukuma\*, H. Ikeda, H. Ishii, S. Kanaeda,  
K. Mori, M. Tejima, M. Tobiya, KEK, Tsukuba, Japan  
G. Bonvicini, H. Farhat, R. Gillard, Wayne State U., Detroit, MI 48202, USA  
G.S. Varner, U. Hawaii, Honolulu, HI 96822, USA

### Abstract

The electron-positron collider KEKB B-factory is currently being upgraded to SuperKEKB. The design luminosity of  $8 \times 10^{35}$  /cm<sup>2</sup>/s will be achieved using beams with low emittance, of several nm and doubling beam currents to 2.6 A in the electron ring (HER) and 3.6 A in the positron ring (LER). A beam position monitor (BPM) system for the HER and LER will be equipped with super-heterodyne detectors, turn-by-turn log-ratio detectors with a fast gate to measure optics parameters during collision operation and detectors of BPMs near the collision point (IP) for orbit feedback to maintain stable collision. New X-ray beam profile monitors based on the coded aperture imaging method will be installed aiming at bunch by bunch measurement of the beam profile. A large angle beamstrahlung monitor detecting polarization of the synchrotron radiation generated by beam-beam interaction will be installed near IP to obtain information about the beam-beam geometry. The bunch-by-bunch feedback system will be upgraded using low noise front-end electronics and new 12-bit iGp digital filters. An overview of beam instrumentation for the SuperKEKB rings will be given in this paper.

### INTRODUCTION

The electron-positron collider KEKB B-factory is currently being upgraded to SuperKEKB[1]. The design luminosity of  $8 \times 10^{35}$  /cm<sup>2</sup>/s will be achieved using the so called nano-beam scheme[2]. Machine upgrades include the replacement of the current, cylindrical LER beam pipes to one with ante-chambers so as to withstand large beam currents and mitigate the electron cloud effect, a new final focus in the interaction region (IR) in order to adopt the nano-beam scheme and the construction of a positron damping ring for positron injection. The first beam is expected in the Japanese FY 2014. Machine parameters of SuperKEKB are shown in Table 1.

### BEAM POSITION MONITOR SYSTEM

The number of beam position monitors (BPMs) in SuperKEKB is 445 in the LER and 466 in the HER. The closed orbit measurement system of KEKB utilized a VXI system[3]. The KEKB detector was a 1 GHz narrowband superheterodyne detector module. One module covered four beam position monitors (BPMs), two in the LER and two in the HER, by multiplexing the signals with switch modules. The main detector system of SuperKEKB follows that of KEKB. The narrowband

\*hitoshi.fukuma@kek.jp

Table 1: Machine Parameters of SuperKEKB

	HER	LER
Energy (GeV)	7	4
Circumference (m)	3016	
Beam current (A)	2.6	3.6
Number of bunches	2500	
Single bunch current (mA)	1.04	1.44
Bunch separation (ns)	4	
Bunch length (mm)	5	6
Beta function @IP hor./ver. (mm)	25/0.30	32/0.27
Emittance (nm)	4.6	3.2
X-Y coupling (%)	0.28	0.27
Vertical beam size at IP (nm)	59	48
Damping time: trans./long. (ms)	58/29	43/22

detectors of KEKB are reused in the SuperKEKB HER. A new narrowband detector with a detection frequency of 509 MHz is being developed, since the cutoff frequency of the new LER ante-chamber is below 1 GHz. Additionally, turn by turn detectors will be installed at selected BPMs at the rate of three per betatron wave length to measure the optics during collision. Also, a special wideband detector is being installed for the four BPMs closest to the collision point (IP) for orbit feedback to maintain stable collision. Table 2 shows a list of detectors in SuperKEKB.

Displacement sensors, which measure the mechanical displacement between a BPM head and a sextupole magnet, are installed at all BPMs neighboring the sextupole magnets, same as at KEKB.

### Button Electrode and BPM Chamber

The BPM chambers and button electrodes in the HER are reused from KEKB. A button electrode with a diameter of 6 mm has been developed for the LER to reduce the beam power at the electrode[4]. The electrode is a flange type for easy replacement and for removal during the TiN coating process of the chamber to reduce the electron cloud. A pin-type inner conductor is used for tight electrical connection. The estimated longitudinal loss factor of a beam chamber with four electrodes is 0.16 mV/pC. The coupling impedance is 2 ohm at the center frequency of 14.8 GHz and the Q value is 38. The estimated growth time of the longitudinal coupled-bunch

Table 2: Detectors for BPM System in SuperKEKB

Type	Resolution	Repetition	Number of units
Narrowband KEKB	2 $\mu$ m	0.25Hz	117
New narrowband	2 $\mu$ m	0.25Hz	127
Turn-by-turn	50 - 100 $\mu$ m	100kHz	270
IR feedback	1 $\mu$ m	5kHz	4

instability is slower than 120 ms at the maximum beam current, which is much longer than the radiation damping time of 43 ms. A prototype was tested successfully at KEKB.

BPM chambers are being fabricated by the KEKB vacuum group. TiN coating and baking of the chambers started this past April.

*Narrowband Detector*

Development of the 509 MHz narrowband detector is in the final stage. A schematic diagram of the detector is shown in Fig. 1. An isolator is put between a selector with PIN-switches and a variable attenuator to reduce the apparent shift of beam position caused by impedance mismatch between the selector and the attenuator. A signal to noise ratio larger than 90 dB was achieved in a laboratory test with CW.

*Turn-by-Turn Detector with Fast Gate*

The schematic diagram of the turn by turn detector is shown in Fig. 2. The detector has GaAs fast gates to select the signal of a non-colliding pilot bunch located typically 6 ns behind a bunch train. Signals of remaining bunches are sent to the output port of the detector, which is connected to the narrowband detector in order to enable a simultaneous measurement of the narrowband detector and the turn-by-turn detector. A glitch cancellation circuit by T. Naito is adopted in the gate circuit to remove switch noise[5]. A 0- $\pi$  splitter and a combiner placed before and after the switches, respectively, remove a common mode glitch of the switches. The turn-by-turn detection is done by a log amp to reduce the cost of the detector. A prototype of the switch was tested at laboratory. The result shows the isolation larger than 85 dB. Also, the detection by the narrowband detector connected to the turn-by-turn detector was not affected by the switches.

*IR Feedback Detector and Processor Unit*

The wideband detector for IR orbit feedback is under development. Vertical positions of both beams are used for orbit feedback to maintain stable beam collision. The orbit shift at the BPMs by a beam-beam deflection is estimated to be several microns. A simulation study shows that the main frequency components due to vibration of the quadrupole closest to the IP are 3, 36 and 53 Hz. Target performance for the development of the

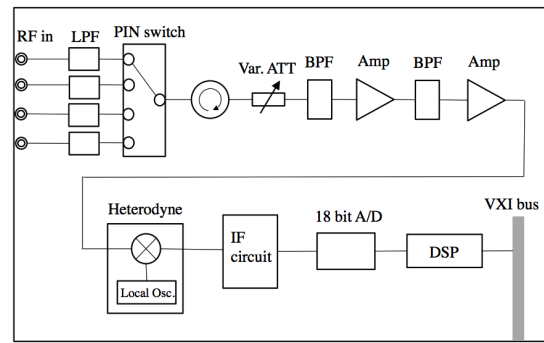


Figure 1: 509 MHz narrowband detector.

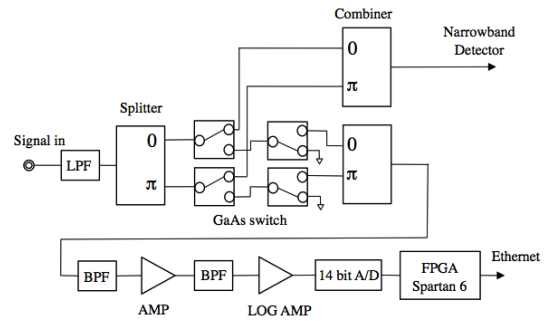


Figure 2: Turn-by-turn detector with fast gate.

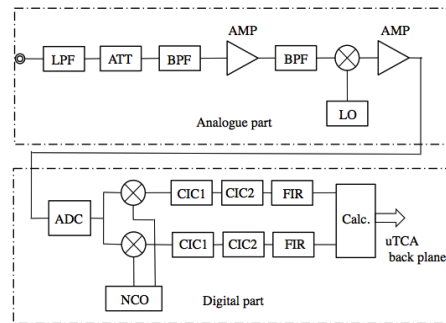


Figure 3: IR feedback detector.

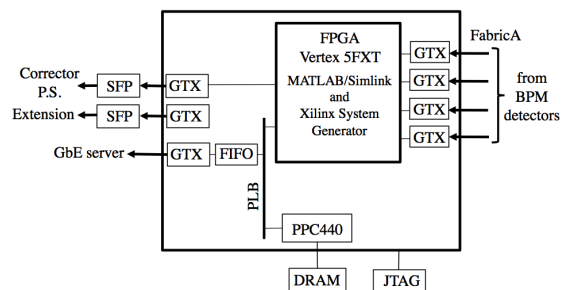


Figure 4: Digital Signal Processor for IR feedback.

detector was tentatively set to a resolution of 1  $\mu$ m and repetition rate of 5 kHz.

The schematic diagram of the detector is shown in Fig. 3. The detector converts the 508.8MHz component to an intermediate frequency (IF) of 16.9 MHz with an

analog mixer to reduce the degradation of the signal to noise ratio by the clock jitter of ADC. The IF signal is digitized by a 16 bit ADC with a sampling rate of 99.4 MHz, then processed by a chain of digital filters (i.e. two CICs and a FIR). The cutoff frequency of the filter is 1 kHz. The digital part is implemented in a micro-TCA board developed for the SuperKEKB LLRF system[6].

A prototype circuit is being tested. Achieved performances of the analogue section are clock jitter of 1.30 ps, noise figure of 14.3dB at 16.9MHz and temperature coefficient of IF-out of -0.03dB/deg. The frequency characteristics of the digital filter was as expected. The position resolution obtained in the test bench is about 50 nm for CW signal. The group delay of the first prototype of the digital filter was 3.3 ms. A simulation shows that the group delay should be less than 1 ms to get enough rejection gain against the disturbance. Taps, i.e. the number of filter coefficients, of the FIR will be reduced to get a shorter group delay.

We are also developing a processor unit for the calculation of the orbit feedback as shown in Fig. 4. The unit has FPGA Vertex 5 on a micro-TCA board. A feedback algorithm is implemented with Matlab/Simulink with system generator (HDL coder) for easy coding.

## SYNCHROTRON RADIATION MONITOR

We will install three kinds of synchrotron radiation monitor: a visible light monitor using an interferometer and a streak camera to measure horizontal beam size and longitudinal beam profile respectively, an X-ray monitor for vertical beam size measurement, and a large angle beamstrahlung monitor to get information on collision status at the IP.

### *Visible Light Monitor*

The large power incident on the extraction mirror is a source of heat-load induced deformations. A source bend in the SuperKEKB LER is a recycled bend in the arc section of SuperKEKB with bending radius twice that of the KEKB source bend. Incident power is less than that of the KEKB HER but more than that of the KEKB LER. The HER bend does not change, and the incident power of 283 W is slightly higher than that of the KEKB HER.

Since the heat deformation was already a great problem at KEKB, it is desirable to have a mirror that does not deform as much under the same heat load. For this reason we are developing diamond mirrors[7]. The mirrors are made of quasi-monocrystalline diamond. A prototype 10 mm x 20 mm x 0.5 mm was completed, and as was one 20 mm x 20 mm x 1 mm. The surface of the mirror is coated by 3  $\mu$ m Au with a thin Cr layer between gold and diamond. The diamond surface is nearly a single crystal, so that good surface smoothness ( $R_a \sim 2$  nm,  $< \sim \lambda/50$ ) is expected. The very good heat conductance and low thermal expansion coefficient reduce the apparent change in magnification, compared to the Be mirrors used at KEKB. A simulation by ANSYS at HER full current shows the magnification error to be 43 % for beryllium

and 3 % for diamond. The deformation of the diamond mirror is being measured in a test bench.

The resolution of the interferometer is fundamentally limited by the wavelength for measurement and by the opening angle between slits which is limited by the antechamber height. A calculation shows that a vertical beam size measurement would be possible with the interferometer, though it is near the limit of the interferometer resolution.

### *X-ray Monitor*

An X-ray beam size monitor will be installed because the interferometer will have marginal vertical resolution and is not capable of single-shot (single bunch, single turn) measurements, which will likely be needed for low-emittance tuning, based on experience at CestrA. The typical vertical beam sizes at the source points in the LER and the HER are 20  $\mu$ m and 10  $\mu$ m, respectively.

We are developing a coded aperture imaging method[8]. This technique was developed by X-ray astronomers using a mask to modulate incoming light. The resulting image must be deconvolved through the mask response, including diffraction and spectral width, to reconstruct the object. An open aperture of 50% gives high flux throughput for bunch-by-bunch measurements. A heat-sensitive and flux-limiting monochromator is not needed. The method has been successfully tested at CestrA[9].

Tests at CestrA showed that a URA (Uniformly Redundant Array) mask gives the predicted single-shot resolution. Two types of URA mask, made of Si and diamond, are considered for use at SuperKEKB, as shown in Fig. 5. A thick Si mask at SuperKEKB full current power load was successfully tested at CestrA. The diamond substrate mask was also fabricated and installed at CestrA and is ready to be tested.

A measurement at the Photon Factory revealed that the Fermionics photon detector had low detection efficiency at high energies due to a small active pixel depth of only 3.5 microns. A simulation estimates single-shot resolution of  $\pm 2.5$ microns at a beam size of 10 microns with this detector. Though this resolution satisfies minimum requirement for SuperKEKB, we are pursuing new detectors which have higher efficiency in the hard X-ray spectrum region and faster response. A trench diode design is being considered as a candidate. The diode has

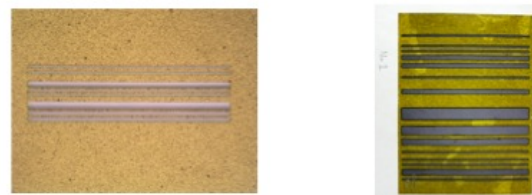


Figure 5: Uniformly redundant array (URA) masks for coded aperture imaging. Left: Gold on a silicon substrate installed at CestrA. Minimum slit width is 5 microns. Right: Gold on a diamond substrate to be tested at CestrA. Minimum slit width is 10 microns.

deep but narrow pixels. The first prototype was fabricated at SLAC and U. Hawaii. The digitizer is the STURM (Sampler for Transients for Uniformly Redundant Mask) ASIC for high-speed readout developed at U. Hawaii. Ver. 1 of the STURM digitizer was tested at the KEK PF in March 2009. A 64-channel system with a Fermionic detector, a preamp board and a STURM digitizer board integrated on a motherboard is being developed for testing at the ATF2[10].

### Large Angle Beamstrahlung Monitor

The LABM is being built in the US, mostly at Wayne State University, with Japanese funding. The device measures the beamstrahlung light emitted at large angle (large compared to the typical  $1/\gamma$  angle of radiation produced by ultra relativistic beams), and relates it to beam parameters so that the beam-beam collision can be optimized for luminosity. Figure 6 shows how polarized light yields measured at specific azimuthal points (in this case, at the top and bottom of the beam pipe, or  $\phi = \pm 90$  degrees) relate to parameters of the beam-beam collision[11].

The deviation of the measured polarization vectors in Fig. 6, with respect to the nominal point for optimal collisions (by construction, the point (1,1)), represents a quantitative measurement of the type of optics present. From the diagram alone, and assuming only one beam needs correction, it is possible to decide which beam needs correction, which type of corrector (dipole, quadrupole or sextupole) to use, and how much correction is needed.

The monitor consists of four viewports, located at the top and bottom of the beam pipe, and respectively at 7 and 8 mrad in the LER and HER. Each viewport is a  $2 \times 2.8 \text{ mm}^2$  primary mirror, reflecting light out of the beam pipe. Light is transported through an optical channel to an optical box (one box serves each side, or two viewports per box), where it is separated into two transverse polarizations and four different wavelength bands, totaling 32 optical and electronic channels. The signal is then counted, time-stamped, and recorded. At full

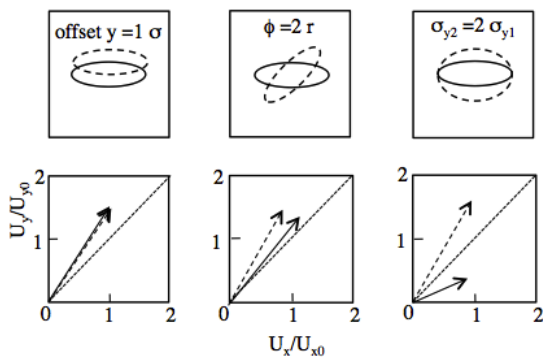


Figure 6: Relation between beam-beam imperfect collisions (top row) and the corresponding large angle beamstrahlung yield, normalized to a calculable quantity  $U_0$ . The beams move in and out of the page.

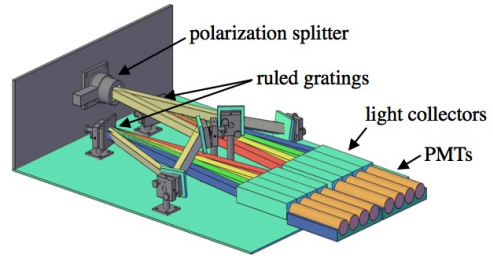


Figure 7: Layout of one half of an optical box. Shown are a polarization splitter, ruled gratings, light collectors and PMTs.

SuperKEKB luminosity, the photon flux at the primary mirror is of the order  $10^{12}$  Hz, and a factor of 50-500 lower for each individual electronic channel.

The design of the device is dominated by control of systematics, based on extensive experience at CESR[12]. Each beam is observed by two viewports located opposite each other, at the azimuth where machine backgrounds are expected to be smallest. Errors due to a misalignment between beam velocity and detector will cancel out when the two signals are summed. Inside the optical box, shown schematically in Fig. 7, the photon counters (typically PMTs) are placed on a small conveyor belt and can be rotated between different optical channels, so that the PMT relative efficiency, which dominates the systematic spectral and polarization error, can be measured online. The replacement of a single ruled grating allows the device to be sensitive to the wavelength ranges 250-500, 300-600, or 450-900 nm.

## BUNCH-BY-BUNCH FEEDBACK SYSTEM

### Transverse Feedback System

Since the horizontal tune is close to a half integer, several turns are needed to observe the orbit change at the monitor if the phase relation between the source of the kick and the monitor is not good. Using two feedback loops with betatron phase advance around 90 degrees might solve this difficulty. For this reason two sets of short stripline kickers which cover two feedback loops with 90 degrees phase difference will be installed in each ring. The phase between the kicker and the monitor is adjusted by the digital filter. The block diagram of the transverse feedback system is shown in Fig. 8.

The monitor chamber has a diameter of 64 mm and the cutoff frequency is 2.7 GHz. The button electrode has a glass feedthrough sealing with low relative dielectric constant of about 4 which has good time and frequency response.

A low-noise front-end for the transverse feedback system is under development. The detection frequency is 2 GHz. A 2 GHz comb filter is used to cut low frequency noise and to improve isolation between bunch signals. A



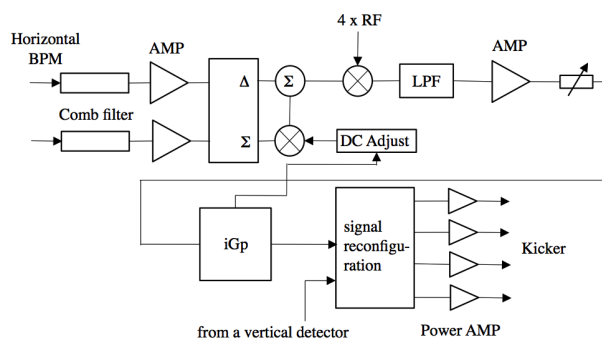


Figure 8: Transverse bunch-by-bunch feedback system.

low noise amp with high IP3 is put immediately after the comb filter. A difference signal is mixed with LO with a frequency of  $4 \times \text{RF}$  frequency, amplified to increase gain, fed to a 600 MHz Bessel LPF, then amplified by a DC amp to improve transient response. Configuration of the amps is being optimized for better gain and noise figure.

Baseline system of the digital filter is the iGp processor developed with SLAC and INFN-LNF supported by US-Japan collaboration on High Energy Physics. It consists of a fast 8-bit ADC, a Virtex-II FPGA with 8 Mbytes of external SRAM, a fast 12-bit DAC and controlled by built-in EPICS-IOC. Since the FPGA is completely programmable, it supports almost any harmonic number, including odd numbers. The iGp was installed at KEKB and tested. It showed excellent performance both in single beam run and in collision runs. The ADC is upgraded to a 12 bit system to extend dynamic range in order to capture the large offset signal due to the beam-beam kick.

The design of the kicker is similar to that of the present kicker. A shunt impedance of 10k ohm per kicker is expected. A feedthrough is changed from 20D type to EIA-7/8 with low loss ceramics. The high-power cables are also changed from 10D to 20D. Power amps are old four 250W-amps and new four 500W-amps in each ring.

### Longitudinal Feedback System

A growth rate of the longitudinal coupled bunch instability due to the impedance of ARES cavities in LER is estimated to be 15 ms which is shorter than the longitudinal radiation damping time. Thus a longitudinal feedback system is indispensable in the LER. The front-end electronics and the digital filters are same as those of transverse system. A digital QPSK modulator is used.

Four DAFNE type kickers with two inputs and two outputs will be installed to get larger capture range. The design of the cavity has started. So far the shunt impedance of 1k ohm at 1.15GHz and the bandwidth of 225 MHz are obtained by a HFSS calculation. Two 500W-amps per kicker are used.

## OTHERS

The tune monitor is reused from KEKB. It is a tracking sweeper with a gate to extract the signal of the pilot

bunch. The oscillation of the pilot bunch is excited by the bunch feedback system with phase locked loop.

The bunch current monitor is revised using a MAX108 8bit ADC and a Spartan6 FPGA in a form of a VME module[13]. Bunch current information will be sent through reflective memory in real time to the bucket selection system during injection.

A DCCT for beam current measurement is reused from KEKB. A loss monitor system consisting of ion chambers and PIN photo-diodes is also reused from KEKB, with an increased number of detectors.

The instrumentations of the damping ring are described briefly. The number of BPMs is eighty-four. Two button electrodes are attached in one flange due to narrow space for their installation. The detector for the BPM is a log-ratio detector accommodated in a VME module. A bunch feedback system is installed to damp the residual bunch oscillation at injection and extraction. The DCCT is reused from KEKB. A measurement room for a synchrotron radiation monitor is located at the tunnel floor level. A streak camera and a gated camera are planned to observe transverse and longitudinal profile.

## ACKNOWLEDGMENTS

The authors would like to thank the KEKB vacuum group for manufacturing BPM chambers. They also thank Prof. J. Fox for valuable advices for the instrumentation system of SuperKEKB. The authors thank staffs at Cornell University for their assistance and efforts for development of the X-ray monitor at CsrTA and Prof. T. Mitsuhashi for cooperation to test the X-ray monitor at ATF2.

## REFERENCES

- [1] H. Koiso, Proceedings of IPAC'11, 1931(2011).
- [2] "SuperB Conceptual Design Report", INFN/AE-07/2, SLAC-R-856, LAL 07-15, March, 2007.
- [3] M.Arinaga et al., Nucl. Instrum. Meth. A499, 100 (2003).
- [4] M. Tobiyama et al., Proceedings of BIW10, 223 (2010).
- [5] T. Naito et al., Proceedings of 6th Particle Accelerator Society Meeting, 88 (2009).
- [6] T. Kobayashi et al., Proceedings of IPAC'12, 3470(2012).
- [7] J. W. Flanagan et al., in these proceedings, TUPB74.
- [8] J. W. Flanagan et al., Proceedings of EPAC'08, 1029(2008).
- [9] J. W. Flanagan et al., Proceedings of IPAC'10, 966(2010).
- [10] J. W. Flanagan et al., in these proceedings, MOPB72.
- [11] E. Luckwald, G. Bonvicini and D. Cinabro, Phys. Rev. E59, 4584(1999).
- [12] G. Bonvicini, ALCPG 2009, Albuquerque, NM, September 2009.
- [13] M. Tobiyama and J. W. Flanagan, in these proceedings, MOPA36.